Ray-Tracing Based Fingerprinting for Indoor Localization

Olivier Renaudin and Thomas Zemen
AIT Austrian Institute of Technology
Donau-City-Strasse 1, 1220 Vienna (Austria)
olivier.renaudin@ait.ac.at

Thomas Burgess
indoo.rs GmbH
Geyschlägergasse 14/2nd floor, 1150 Vienna (Austria)
thomas@indoo.rs

***Abstract*—Empirical fingerprinting is currently one of the most efficient localization methods in indoor environments, due to the now ubiquitous deployment of wireless local area networks. A fingerprint is the pattern of received signal strengths from all the access points visible at a particular position. Reference fingerprints are obtained from extensive measurement campaigns and used during an offline phase to construct suitable radio maps of the environment of interest. However, this approach is very site-specific and the radio maps require therefore to be regularly updated in order to take into account changes in the environment, i.e. a labor-intensive and time-consuming task.**

Hence, ray-tracing simulations are instead used in this paper to construct these radio maps based on deterministic prediction of the radio wave propagation. To validate this approach, field experiments were conducted in an indoor office environment. The results show *(i):* the sensitivity of fingerprints to small-scale fading and human shadowing, as well as *(ii):* good agreement between the measured and ray-tracing simulated fingerprints, especially with strong line-of-sight.

I. Introduction

Outdoor localization is often based on the global positioning system (GPS), with satisfactory performance results when the signals from three satellites or more can be successfully decoded at the receiver side. However, this approach cannot be extended to the development of suitable indoor positioning systems (in terms of performance, efficiency and reliability), owing to the strong attenuation of the GPS signal caused by the walls and the structure of the buildings.

As a result, other wireless technologies have to be considered, among which Bluetooth Low Energy (BLE) currently seems to be the most promising [1]. It is based on small size, light weight, low cost, power saving (hence easily deployable) beacons. BLE operates in the unlicensed 2.4 GHz ISM band (also used by WiFi) and consists of 40 channels, each 2 MHz wide (i.e. much narrower than the 20 MHz of WiFi access points), among which 37 are used for the exchange of data among paired devices, whereas the 3 other ones (labeled 37, 38 and 39) are used for broadcasting advertisement messages. These channels are widely spaced at 2402 MHz, 2426 MHz and 2480 MHz, respectively, i.e. possibilities of interference with already deployed WiFi systems are minimized.

The advertisement packets are unsolicited and typically have very short duration and minimal overhead to save on power consumption. They are broadcast repetitively at a predefined advertising rate while hopping over the 3 designated channels [1]. The received signal strength (RSS) from either advertisement channel can be opportunistically used as a fingerprint corresponding to the current position of the user's terminal. Localization is then achieved by comparing online the fingerprint measured on the user's terminal to the reference radio map of the environment [2]–[6]. Accurate radio maps are thus crucial to achieve good localization performance in complex indoor environments. This is up to now usually done (in both academia and industry) by repeating measurement campaigns on a regular basis, what is labor intensive, time and resource consuming, and ultimately expensive.

To alleviate these limitations, ray-tracing (RT) simulations can be used in order to predict these fingerprints [7], [8]. The radio wave propagation (i.e. all the propagation paths) between a pair of transmitter (Tx) and receiver (Rx) are calculated deterministically based on the geometrical (optics-based) theory of propagation [9]–[11]. Their non-coherent superposition at the Rx side yields therefore the reference RSS which should be observed at this position in the environment for a given BLE beacon. RT simulations are known to be able to achieve high accuracy levels, though at the cost of a detailed description of the propagation environment (e.g. environment geometry, electromagnetic properties of the materials, etc.) and a high computational complexity [10], [11]. Hence, the main channel characteristics have to be identified in order to simplify the complexity of RT simulations while keeping high performance levels in terms of RSS fingerprint prediction. The scientific contributions in this paper are two-fold, namely

- A detailed comparison between measured and RT simulated RSS fingerprints in an indoor office environment,
- The identification of the most significant radio wave propagation mechanisms for accurate estimation of the RSS fingerprints.

The remainder of this paper is organized as follows: Section II introduces the RT simulation tool, including the description of the indoor office environment and of the main radio wave propagation mechanisms. Section III evaluates the measured and RT simulated RSS fingerprints, which are compared in terms of received power and large-scale fading. Their sensitivity to small-scale fading is also investigated. Finally, Section IV provides a summary and a concluding discussion.

978-1-5386-3512-4/18/$31.00 ©2018 IEEE

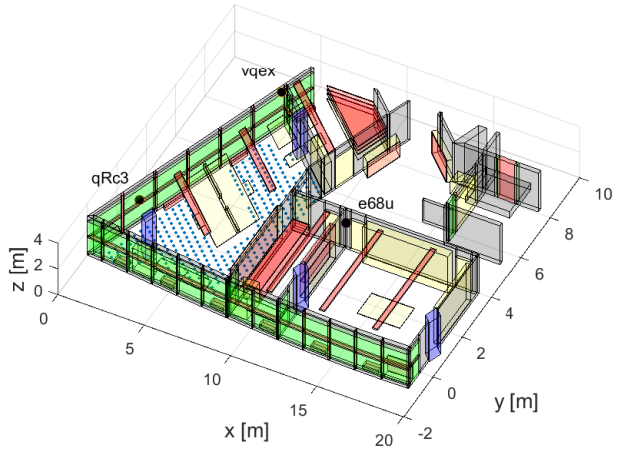

Fig. 1. Floor plan of the indoor office environment. Concrete, glass, metal, wood and plaster furniture or elements are represented here in blue, green, red, yellow and black blocks, respectively. The blue dots correspond to the Rx positions where the RSS fingerprints are measured and simulated.

II. Ray-Tracing Simulation Model

A. RT Scenario

RT simulations have been conducted in an indoor office environment whose partial 3-dimensional (3D) floor map is shown in Fig. 1, and more specifically inside the office at the bottom left corner, whose dimensions are approximately 8.5 m $\times 8.0$ m $\times 3.0$ m.

The inner walls and ceiling are made of drywall, whereas the outer ones are glass windows with metallic frames. Concrete pillars are visible and portions of the inner walls between adjacent offices are left open and installed with glass windows. The rooms are filled with furniture (including wooden desks and shelves, metallic wall units and lighting, etc.) and equipment. The environment is modeled using non-overlapping quadrangular parallelepiped blocks which are assigned 3D Cartesian coordinates and homogeneous electromagnetic properties. The values of relative permittivity ϵ_r and conductivity σ are set as follows: $\epsilon_r = 4$ and $\sigma = 0.02$ S/m for drywall, $\epsilon_r = 6$ and $\sigma = 0.01$ S/m for concrete, $\epsilon_r = 3$ and $\sigma = 1 \times 10^{-9}$ S/m for glass, $\epsilon_r = 2.1$ and $\sigma = 0.05$ S/m for wood. Metallic blocks are considered as perfect electric conductors, i.e. with $\epsilon_r = 1$ and $\sigma = 1 \times 10^7$ S/m.

Three BLE beacons are considered at the Tx side. They are located as shown in Fig. 1, i.e.

- On the second window starting from the bottom left corner of the office (beacon name: qRc3), at coordinates: $[x_{\text{qRc3}} = 1.32\ ;\ y_{\text{qRc3}} = 2.00\ ;\ z_{\text{qRc3}} = 1.80]$ m,
- On the wall above the last window in the top left corner of the office (beacon name: vqex), at coordinates: $[x_{\text{vqex}} = 4.64\ ;\ y_{\text{vqex}} = 7.81\ ;\ z_{\text{vqex}} = 2.75]$ m,
- On the wall in the corridor between the office and the workshop next door (beacon name: e68u), at coordinates: $[x_{\text{e68u}} = 11.60\ ;\ y_{\text{e68u}} = 3.99\ ;\ z_{\text{e68u}} = 1.80]$ m.

TABLE I
RT simulation parameters

Parameter	Value
Carrier frequency f_c	2.4 GHz
Bandwidth B	2 MHz
Number of Rx positions N	318
Grid sampling resolution $d_x = d_y$	0.30 m
Tx/Rx antenna radiation patterns	Omni-directional

The two first positions ensure that the Rx is always placed in strong line-of-sight (LOS) conditions, whereas the third one yields mostly non-line-of-sight (NLOS) conditions inside the office. For each BLE beacon, the RSS fingerprints were measured and simulated at $N = 318$ points spaced $d_x = d_y = 0.30$ m apart one from another in each direction. Their ground-truth positions are indicated in Fig. 1. The mobile phone is assumed to be held horizontally in the user's hand, about 1.20 m above the floor level.

B. RT Channel Model

Three radio wave propagation mechanisms are taken into account in RT, namely *(i):* LOS, *(ii):* specular reflection and diffraction, as well as *(iii):* diffuse scattering.

The LOS and the specular contributions are evaluated using both geometrical optics and the uniform theory of diffraction [10], [11], with reflections up to the third order and single bounce diffraction. On the other hand, the diffuse scattering components are assumed to be single bounce, with the reflection contribution occurring either first (i.e. diffuse scattering as last interaction, LDS) or last (i.e. diffuse scattering as first interaction, FDS). Penetration and wall transmission are both embedded in these propagation mechanisms, since indoor environments are considered.

As a consequence, the propagation path and complex electric field of all the contributions can be calculated given the geometrical and electromagnetic description of the environment [9], [11]. The Tx and Rx antenna radiation patterns must also be taken into account and will be assumed omnidirectional both in azimuth and in elevation. All the simulation parameters are summarized in Table I. Fig. 2 shows all the contributions obtained by RT between the BLE beacon qRc3 and one Rx position in the indoor office environment.

More detailed information about this RT simulation tool can be found in [10]–[12] for descriptions of the underlying physical concepts and in [11], [13] for the corresponding numerical implementation issues, respectively.

C. RT Simulated RSS Fingerprints

Assuming infinite bandwidth, the complex impulse response (IR) of the channel is defined as the superposition at the Rx side of the L path contributions identified by RT, i.e.

$$h(\tau) = \sum_{l=1}^{L} \eta_l e^{j\phi_l} \delta(\tau - \tau_l), \tag{1}$$

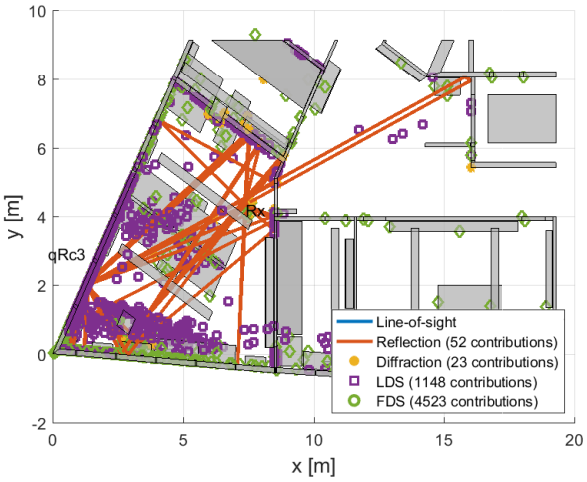

Fig. 2. Contributions of the different radio wave propagation mechanisms between the BLE beacon qRc3 and one position in the office.

where τ_l, η_l and ϕ_l are the delay, gain and phase of the l^{th} propagation path, respectively. The IR is in practice bandlimited: the IR in (1) is indeed convolved with a pulse-shaping raised cosine filter $g_m(\tau)$ with roll-off factor $\alpha = 0.4$ and bandwidth $B = 2$ MHz [1] and it is then sampled at uniform time intervals $\Delta\tau = k/B$, where $k = 0, \ldots, K-1$. In the following, the RSS will be assumed to be defined as

$$\text{RSS} = \left| \sum_{k=0}^{K-1} \sum_{l=1}^{L} \eta_l e^{j\phi_l} \int_{-\infty}^{+\infty} g_m(\tau - k\Delta\tau - \tau_l)\, d\tau \right|^2, \quad (2)$$

since the BLE standard does not specify how it is calculated. It can change from device to device and this information is usually not made available by manufacturers.

III. Experimental Results

A. Measurement Set-Up

The BLE beacons are manufactured by kontakt.io[1] and are placed inside the office as shown in Fig. 1. Their advertising rate and transmission power are set to 350 ms (i.e. 2.85 Hz) and $+4$ dBm, respectively.

A Nexus 5.X smartphone (Android version 7.1.2) was used in order to measure the RSS fingerprints, with the BLUES application developed by indoo.rs. They were recorded at the same positions where the RT simulations were conducted, over a 5 s time interval repeated 3 times in order to average out small-scale fading and to have enough samples for estimating reliable statistics. Each RSS value is associated with the BLE beacon from which the advertisement signal is received, but the corresponding channel is not known.

[1]More information about their technical specifications can be found here: https://store.kontakt.io/our-products/30-double-battery-beacon.html

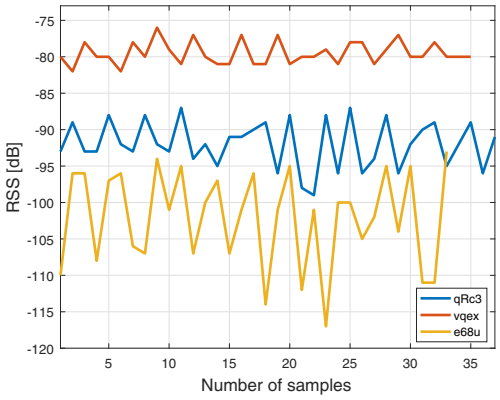

Fig. 3. Variability over time of the RSS fingerprints measured at one Rx position inside the office for the three BLE beacons.

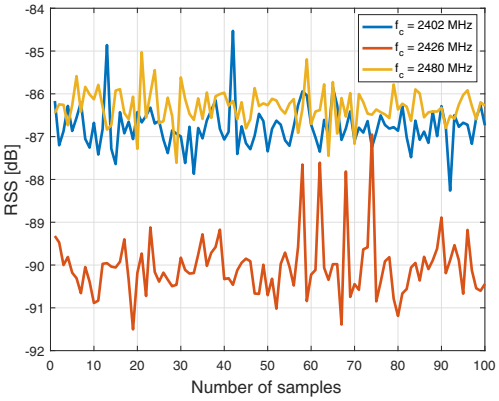

Fig. 4. Variability over time and frequency of the RT simulated RSS fingerprints at the same position as in Fig. 3 for the BLE beacon qRc3.

B. Small-Scale Fading of the RSS Fingerprints

Fig. 3 shows an example of RSS fingerprints recorded for the three BLE beacons at one position, when the advertisement channel is not reported by the Rx terminal. Deep fades up to 10 to 20 dB can then be observed, owing to *(i):* the non-constant antenna gain of the BLE beacons over frequency, and *(ii):* the constructive or destructive interferences depending on the center frequency of the channel on which the advertisement signal is received. Similar observations have already been reported in [14], but Fig. 4 shows that a similar behavior can also be reproduced in RT simulations, where the difference between the RSS values of the three advertisement channels can be up to 3 to 5 dB. Note that the fading which is observed for the RSS values is due to the stochastic modeling of the diffuse scattering in the RT simulations [11].

The RSS fingerprints exhibit therefore artificially high noise levels and significant fluctuations over time even in a fully static environment, as if they were drawn randomly from one of the three BLE advertisement channels. Such small-scale fading occurs over distance ranges much shorter than the expected accuracy of indoor localization systems based on RSS fingerprints and may dramatically affect their performance if

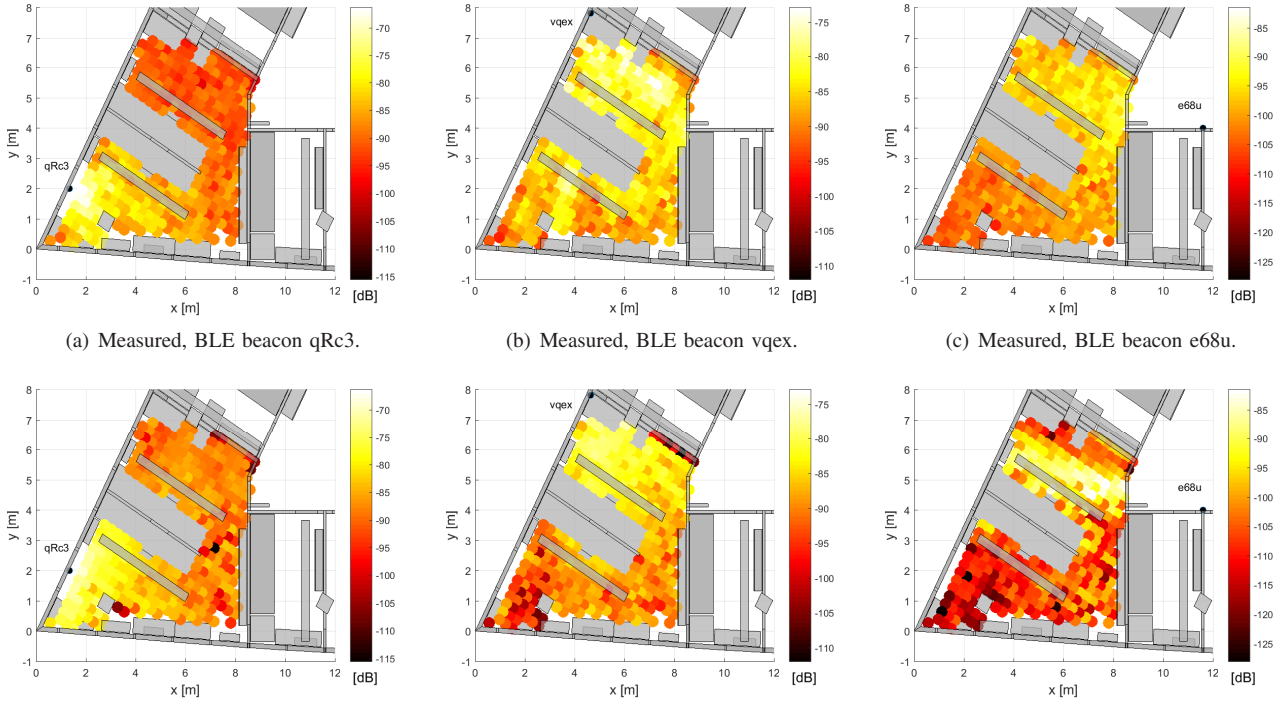

(a) Measured, BLE beacon qRc3. (b) Measured, BLE beacon vqex. (c) Measured, BLE beacon e68u.

(d) RT simulated, BLE beacon qRc3. (e) RT simulated, BLE beacon vqex. (f) RT simulated, BLE beacon e68u.

Fig. 5. Spatial distributions of the measured and RT simulated RSS fingerprints in the office for the three BLE beacons, respectively.

it is not carefully taken into account when creating the RSS fingerprint radio map of the environment.

C. RSS Fingerprint Maps

Fig. 5 shows the spatial distribution of the average measured and RT simulated RSS fingerprints for the three BLE beacons in the office, respectively. A very good agreement can typically be observed for positions with strong LOS conditions. However, significant discrepancies between measurements and RT simulations can occur when the LOS is obstructed. In that case, RT simulated RSS fingerprints are indeed smaller than the measured ones, possibly by 10 to 20 dB as for the BLE beacon e68u, e.g. owing to the simplified description of the indoor office environment. This has no impact in strong LOS conditions (since the LOS component then dominates all the other contributions), but yields otherwise significant prediction errors between the measured and RT simulated RSS fingerprints, when the radio wave propagation between the Tx and Rx sides relies on these mechanisms.

The RSS can be modeled as decaying linearly (in the dB scale) with the distance d between a BLE beacon and a reference position, such that

$$RSS_{[\text{dB}]} = RSS_{0,[\text{dB}]} + 10\eta \log_{10}\left(\frac{d}{d_0}\right) + S_{\text{LS},[\text{dB}]}, \qquad (3)$$

where η and $RSS_{0,[\text{dB}]}$ denote the exponent and the RSS at a reference distance ($d_0 = 1$m), respectively. On the other hand, the large-scale fading $S_{\text{LS},[\text{dB}]}$ describes the fluctuations of the channel gain over large distances and is usually modeled as a Gaussian random process with zero-mean and standard-deviation $\sigma_{[\text{dB}]}$.

TABLE II
RECEIVED POWER AND LARGE-SCALE FADING PARAMETERS FOR THE MEASURED / RT SIMULATED RSS FINGERPRINTS.

	$\eta_{\text{meas / RT}}$	$RSS_{0,[dB],\text{meas / RT}}$	$\sigma_{[dB],\text{meas / RT}}$
qRc3	-1.99 / -1.93	-74.42 / -73.30	3.16 / 4.10
vqex	-1.46 / -2.35	-71.04 / -70.79	3.49 / 4.39
e68u	-1.93 / -2.97	-83.44 / -79.45	2.92 / 8.38

Table II shows that the measured and RT simulated RSS fingerprints yield very similar parametrization of the model in (3) either under strong LOS conditions (i.e. for BLE beacons qRc3 and vqex) or when both LOS and NLOS conditions are experienced depending on the position in the office where the RSS fingerprint is recorded (i.e. for BLE beacon e68u), with in all cases almost free-space radio wave propagation (i.e. $\eta \approx 2$). Note also that the measured and RT simulated RSS fingerprints have the same spatial distribution inside the office. However, larger discrepancies can be observed in the large-scale fading for BLE beacon e68u, meaning that RT simulated RSS fingerprints may be subject to larger fluctuations around their actual values in NLOS conditions.

IV. CONCLUSION

In this paper, RT was used in order to predict the RSS fingerprints and to generate the radio map of an indoor office

environment for BLE based localization systems. Measured and RT simulation results both show that RSS fingerprints are highly dependent on the frequency of the advertisement channel from which they are reported. Moreover, a very good agreement can be observed between measured and RT simulated RSS fingerprints, especially in LOS conditions. NLOS situations yield however significant discrepancies, owing to radio wave propagation mechanisms not yet taken into account in the RT simulations.

Future work will consist in comparing the measured and RT simulated RSS fingerprints in terms of localization performance. We will also focus on reducing the complexity of the RT simulation tool while keeping very good prediction accuracy of the RSS fingerprints. Finally, this approach will be extended to more complex indoor environments, where a larger number of BLE beacons is being deployed.

ACKNOWLEDGMENT

This work is supported by the Austrian Research Promotion Agency (FFG) and the EUROSTARS program in the project AGENT. This work has been performed under the framework of COST Action CA15104, Inclusive Radio Communication Networks for 5G and beyond (IRACON).

REFERENCES

[1] *Bluetooth Core Specification Version 5.0*, Kirkland (WA, USA), December 2015, 10.1109/IEEESTD.2011.5712769.

[2] H. X. Liu, B. A. Chen, P. H. Tseng, K. T. Feng, and T. S. Wang, "Map-aware indoor area estimation with shortest path based on RSS fingerprinting," in *81st IEEE Vehicular Technology Conference (VTC)*, Glasgow (Scotland), May 2015, pp. 1 – 5.

[3] V. Honkavirta, T. Perälä, S. Ali-Löytty, and R. Piché, "A comparative survey of WLAN location fingerprinting methods," in *6th Workshop on Positioning, Navigation and Communication (WPNC)*, vol. 3, Hannover (Germany), March 2009, pp. 1283 – 1288.

[4] C. Wu, Z. Yang, Y. Liu, and W. Xi, "WILL: Wireless indoor localization without site survey," *IEEE Transactions on Parallel and Distributed Systems*, vol. 24, no. 4, pp. 839 – 848, April 2013.

[5] P. H. Tseng, Y. C. Chan, Y. J. Lin, D. B. Lin, N. Wu, and T. M. Wang, "Ray-tracing-assisted fingerprinting based on channel impulse response measurement for indoor positioning," *IEEE Transactions on Instrumentation and Measurement*, vol. 66, no. 5, pp. 1032 – 1045, May 2017.

[6] C. Wu, Z. Yang, and C. Xiao, "Automatic radio map adaptation for indoor localization using smartphones," *IEEE Transactions on Mobile Computing*, vol. PP, no. 99, pp. 1 – 1, August 2017.

[7] J. Neburka, Z. Tlamsa, V. Benes, L. Polak, O. Kaller, L. Bolecek, J. Sebesta, and T. Kratochvil, "Study of the performance of RSSI based Bluetooth smart indoor positioning," in *26th International Conference Radioelektronika (RADIOELEKTRONIKA)*, Kosice (Slovakia), April 2016.

[8] J. Pelant, Z. Tlamsa, V. Benes, L. Polak, O. Kaller, L. Bolecek, J. Kufa, J. Sebesta, and T. Kratochvil, "BLE device indoor localization based on RSS fingerprinting mapped by propagation modes," in *27th International Conference Radioelektronika (RADIOELEKTRONIKA)*, Brno (Czech Republic), April 2017.

[9] C. Oestges, B. Clerckx, L. Raynaud, and D. Vanhoenacker-Janvier, "Deterministic channel modeling and performance simulation of microcellular wide-band communication systems," *IEEE Transactions on Vehicular Technology*, vol. 51, no. 6, pp. 1422 – 1430, November 2002.

[10] F. Mani, "Improved ray-tracing for advanced radio propagation channel modeling," Ph.D. dissertation, Université catholique de Louvain, 2012.

[11] M. Gan, "Accurate and low-complexity ray tracing channel modeling," Ph.D. dissertation, Technische Universität Wien, 2015.

[12] M. Gan, X. Li, F. Tufvesson, and T. Zemen, "An effective subdivision algorithm for diffuse scattering of ray tracing," in *XXXIst URSI General Assembly and Scientific Symposium (URSI GASS)*, Beijing (China), August 2014, pp. 1 – 4.

[13] X. Li, "Efficient ray tracing simulation," Master's thesis, Lund University, 2014.

[14] R. Faragher and R. Harle, "An analysis of the accuracy of Bluetooth low energy for indoor positioning applications," in *27th International Technical Meeting of The Satellite Division of the Institute of Navigation (ION GNSS+)*, Tampa (FL, USA), September 2014, pp. 201 – 210.